Reactionless Propulsion

Randell Lee Mills[a*], D. Hsieh[a], K. Sadman[a]
[a] Brilliant Light Power, Inc., 105 Terry Drive, Suite 103, Newtown, PA 18940

Abstract

A special exception to Newton's third law, not considered by Newton, was the absorption of a photon by a free electron moving with positive velocity relative to its absolute-space inertial frame of reference, the frame corresponding to the creation of the electron at rest (i.e. zero kinetic energy above its exact photon production energy). Absolute space conserves the mass-energy inventory of the universe. Conservation of energy and angular momentum of the photon and electron that absorbs the photon requires the photon and its energy transition to the electron at an increased kinetic energy in the initial direction of travel. The transition is reactionless due to the object of reaction being spacetime that propagates the photon. This phenomenon called space drive provides a mechanism for a reactionless propulsion system. Using space drive, the plasma confinement was achieved which is also shown to be the mechanism of the confinement of plasma outside of flattened waveguide and microwave cavity sources of atmospheric pressure plasma jets. Jets spanning lengths that are 100,000 times higher than possible based on the limiting recombination lifetime of plasma in the absence of microwave power to maintain them is shown to be due to space drive. Moreover, the plasma sound speed and plasma pressure were determined using plasma electron density and temperature measurements, and it was observed that the plasma pressure was made directional by space drive with agreement between corresponding calculated and experimentally observed extent of confinement of powerless plasma jets and the maximum lift capability of space drive. Specifically, the observation of supersonic propagating lift of over 46.9 kg (103.3 lbs.) with 330 W of microwave power applied for 40 ms corresponding to 13.2 J is reported. The measured lift for energy absorbed matched physical predictions. This first-of-a-kind space drive prototype demonstrated a weight to power ratio lift capability of about 3 W/lbs. which compares very favorably to that of Starship of 655,000 W/lb.

Introduction

The nature of absolute space for the proper time and mass/energy of a fundamental particle such as a free electron and the constant maximum speed of light give rise to a reactionless means of propulsion involving conservation of photon energy absorbed by a free lepton such as a free electron. Conservation laws of a fundamental particle such as a free electron during photon absorption results in the directional increase in the inertial parameters of inertial momentum and mass/energy corresponding to kinetic energy with no reaction of a massive third body reaction partner in the exchange. Specifically, an incident photon increases the kinetic energy of a free electron in the direction of it motion relative to its absolute space by ½ of the photon energy given by $\hbar\omega$ wherein $\hbar$ is Planck's constant bar and ω is the photon angular frequency. All electromagnetic waves comprise a superposition of photons [1]. Transfer of photon energy must instantaneously obey causality, locality, continuity with conservation of photon energy of $\hbar\omega$ and the electron and photon angular momentum $\hbar$, wherein conservation of linear momentum is not obeyed. The classical theory regarding the nature of the photon and free electron that give rise to the reactionless force exploited as the mechanism a novel means of propulsion called "space drive" is given in by Mills [1]. A simulation of this phenomenon is given by Mills [2]. The nature of absolute space a corresponding Lorentz frame transforms are given by Mills [3].

Typically, there is no directional flow in microwave plasmas. The vector acceleration and gained electron kinetic energy caused by absorption of microwave power averages out to zero net flow due to the random motion of the plasma electrons. Only heating occurs which is average kinetic energy. Space drive requires first the creation of a directional electron flow such that microwave absorption increases the directional electron kinetic energy and plasma flow. The gained kinetic energy is relative to the electron's absolute space frame, the rest frame of the creation of the electron at its particle production event. To conserve the mass-energy inventory of the universe, the electron inertial frame cannot be relative/arbitrary [3].

Free electrons can also directionally and reactionlessly absorb laser light. This is the mechanism of laser electron accelerators wherein photons are absorbed by the free electrons of highly ionized plasmas such as hydrogen plasmas of an open hydrogen gas jet [4]. The electrons are reactionlessly and directionally accelerated to relativistic energies. The propagation direction of a high-power laser pulse (e.g. 0.5TW) in the gas establishes the vector of directionality of the reactionless electron acceleration. Relativistic protons beams may also be created by ion dragging [5]. Some limitations of a laser reactionless space drive are the high power required, large scale of the laser system, laser power inefficiency, small cross sectional beam size, and cost.

Cross-section for visible photon absorption by free electrons is very low compared to that for microwave photons wherein it as well well-known that essentially all the power of microwave plasma is absorbed by free electrons, but since the electrons have a random velocity, no space drive effect is typically observed since any increase in kinetic energy in any initial random direction of motion will be randomized to be non-directional. With the establishment of a slight plasma flow bias by maintaining a corresponding plasma gas flow bias, a very small excess of electrons each having a maximum velocity projection in a selected direction (e.g. vertical) absorbs microwave photons to increase the vertical directionality of the electron velocities in a positive feedback mechanism to rapidly organize the plasma electrons into a full directional electron flow that becomes a directed plasma flow due to ion dragging.

Directional kinetic energy may be manifest as a directional lift force by directing the kinetic energized electrons toward a transducer. In two patent applications Mills [6-7] discloses space drive, a system that exploits conversion of photon energy (e.g. microwave photons) into reactionless free electron kinetic energy to provide reactionless lift and propulsion. Specially, space drive comprises (i) a source of microwave power such as microwave generator and a matching network, (ii) a plasma torch with a directional plasma gas flow along the axis of a plasma chamber tube that is powered by the microwave power to maintain a plasma comprising a flow of free electrons along the axis of the plasma tube, (iii) a source of microwave photons such a magnetron and an antenna to apply microwave power to the directional electron flow to create (a) an increase in kinetic energy in the directional electron flow due to the free electrons absorbing the microwave photons in a directional manner and gaining reactionless kinetic energy in a directional manner and (b) directional plasma gas flow with increased kinetic energy since the electrons drag positive ions and further accelerate the collisionally-coupled neutral plasma gas, and (v) a transducer (e.g. plasma-flow-arresting magnetohydrodynamic generator) to convert the directional increased kinetic energy flow into a lift force.

In general, the plasma may be formed by a plasma generator such as a surfaguide plasma generator such as exemplary one by Sairem [8]. Alternatively, the plasma generator may comprise a microwave plasma system such as an atmospheric-pressure microwave plasma generator. An exemplary atmospheric-pressure microwave plasma generator is one by Leins et al. [9]. A commercial version is available by Muegge Gerling [10]. Microwave plasma thrusters that function on the principle of reactive momentum conservation between an object to be propelled and a kinetic energized stream of gas and ions have been studied extensively. The reactive propulsion force and thrust and corresponding efficiency produced by flowing and expanding a pressurized plasma gas energized by microwave power through a typical converging-diverging nozzle such as de Laval nozzle has been shown to be poor.

Motivated by the desire to replace jet engines based on fossil fuels Ye et al. at Wuhan University [11] tested an atmospheric-pressure microwave plasma torch for the ability to heat an ambient air stream and create a pressure and corresponding lifting force on a weight comprising a metal ball of adjustable mass that occluded microwave heated plasma torch gas flow at the top of the torch plasma tube when the gravitational force on the ball or weight matched the lifting force of the microwave heated flowing gas. The lift was assigned to microwave thermal heating of the air in addition to the baseline pressure above atmospheric to maintain a selected flow rate in the range of 0.7 to 1.45 m^3/h. Ye et al. [12] calculated a corresponding pressure from the weight lifted which showed that about 11% of the applied microwave power heated the gas. Ye et al. [11] equated the internal static pressure of the heated air to propulsive thrust [11,12,13]. Unfortunately, the upward force of the of pressurized gas on the ball and the force of the ball's weight are equal and in opposite directions. The pressure forces on the plasma tube also balance. There was no net propulsion force on the plasma tube, ball, and plasma tube. A net propulsion force in the opposite direction of the ball-restricted plasma tube is given by the nozzle trust equation wherein any net thrust was due to the gases escaping through the small aperture between the ball surface at the top surface of the plasma tube. This thrust is orders of magnitude less than the lift force due to the pressure and flow of the plasma torch plasma gas when the proper nozzle thrust physics was applied to the data as reported in an analysis of the Ye at al. experiment [11] by a Wright et al. at the University of California Los Angeles [13].

Currently all such propulsion systems are based on production of equal and opposite reactive momentum transfer that requires system mass loss in addition to highly inefficient power loss. In contrast, space drive lift or thrust is in the direction of mass flow (i.e. plasma flow), requires no mass loss, and can be 70% or more power efficient of microwave power to propulsion kinetic power, wherein the efficiency can be boosted by energy recovery in a closed system. Thus, it is worth revisiting the analysis of the Ye at al. [11] experiment in these terms since some of the basic components of space drive are present assuming that the flattened microwave waveguide was capable of supplying microwave photons corresponding to a far field effect in addition to free electrons via gas ionization which may be predominantly via near electric field coupling (e.g. collisional or ohmic power transfer).

Plasma Jet Experiments

The experiments of Ye et al. [11] were repeated using an Astex microwave system to maintain an atmospheric pressure plasma torch extending outside of a flattened waveguide comprising (i) Model AX2115 1500W Microwave Power Generator Serial 347, (ii) Model SXRHA Magnetron Serial 329, (iii) Model AX3030 Isolator Serial EO380. (iv) Model AX 3120 Circulator cooled by a bath recirculating water cooling laboratory chiller VEVOR 6L, 800W, a power meter Serial EO522, and Model AX3041 Three Stub Tuner Serial 0757. The dimensions of the flattened copper waveguide were 576.7 mm length, 34.04 mm height, 72.14 mm width, and a height of 17.02 mm at the flatted section. The center of the flatten section had a 23.37 mm circular hole on top and bottom surfaces to allow for the insertion of the 23 mm OD 3 mm thick quartz plasma tube. A Tesla coil was used as the plasma igniter. The near atmospheric pressure gas was supplied by a constant pressure flow controller (Alicat Scientific M-50SLPM-D-DB9M/5M, Gas: Air, Range (33.3 SLPM), P2: 14-20 PSIA) that was set to provide the desired initial flow rate at constant pressure. 4 mm OD stainless steel (SS) balls were inserted through a 6 mm hole in a 75.5 mm OD steel hollow wherein the SS ball were added to the limit of the maximum weight that suppressed the ball from vibrating due to a balance between the lift and the force of gravity on the ball.

It was found that adding weight to the 75.5 mm steel ball by addition of small metal balls caused the plasma to extinguish due to the fast response time of the Alicat MFC to maintain constant pressure. This was apparently not an issue for Ye et al. [11] wherein an air compressor and a pressure regulator were used to provide constant pressure. In the latter case, the response time to transient interruptions in plasma gas flow would be expected to be much slower. The Alicat constant pressure flow controller was replaced with a gas pressure regulator (VWR Scientific, Cat. No. 55850 225) connected to a tank of air. The 10 $slmin^{-1}$ flow was measured with a gas flow meter (Cole Palme PMR 1-01565), and the lift without microwave power was measured to be 0.3 lbs. (0.136 kg). With a microwave input power of 400W, the lift was measured to be 0.5 lbs. (0.227 kg) corresponding to a net lift over the lift to maintain plasma flow of 0.2 lbs. (0.091 kg) which matches the net 0.092 kg recorded at 400W and 0.6 m^3/h flow rate by Ye et al. [11]. The measured lift was significantly less than the lift of 0.35 kg calculated from the plasma pressure which is likely due to measuring the lift at the top of the plasma tube after most of the lift was lost to space drive de-excitation along the plasma jet height (Figure 1). The present waveguide was more tapered than that of Ye et al. [11] which may have affected the lift wherein the volume sufficient to provide the equivalent of free-space photons was slightly reduced as discussed in the Lift Experiments section. By selecting a cavity to predominantly produce free-space microwave photons and a plasma gas to increase the electron density, a lift of 46.9 kg was produced for only 330W input as given in Table 2, corresponding to a power corrected gain of 625 times the waveguide lift.

Figure 1. Height of atmospheric plasma jet launched by a flattened-waveguide atmospheric pressure air plasma jet as the microwave power was varied reported by Ye et al. [12].

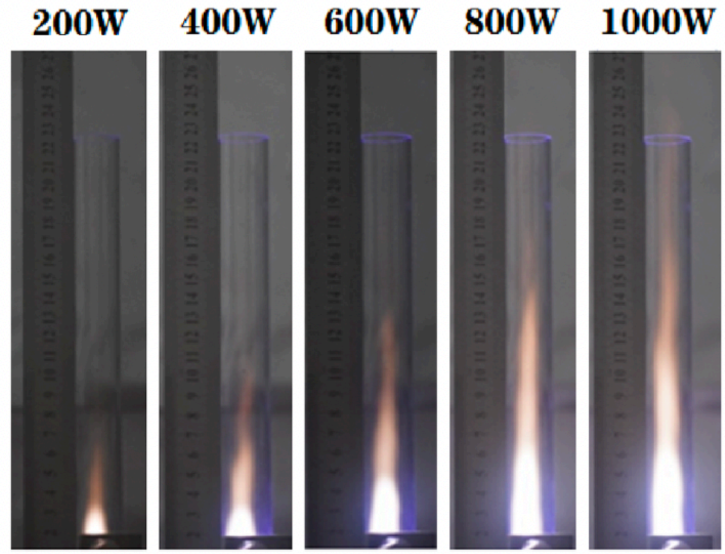

In addition to measuring the lift using a 75.5 mm OD steel hollow ball, Ye et al. [11] reported plasma jets that extended up to 600 mm from the flattened waveguide launcher as shown in Figure 1. The technology of plasma jets from flattened waveguides is well established. Microwave torch cavity-launched plasma jets are common as well as shown in Figure 2 wherein the Leins et al. [9] reported plasma jets in air that extended up to 564 mm outside the cavity. Atmospheric air plasma jets extending 438 mm outside of the waveguide were reproduced in this study (Figure 3) wherein the experiments and analysis were directed to the mechanism of the jet. Specifically, the mechanism of the plasma jet that was continuously maintained outside of the waveguide launcher and the height of the jet with the variation of the power delivered to the plasma and the flow rate of the plasma gas was determined.

Figure 2. Height of atmospheric plasma jet launched by microwave cavity as the microwave power and plasm gas flow rate were varied reported by Leins et al. [9]. (This figure is adapted from Leins, M., Gaiser, S., Schulz, A., Walker, M., Schumacher, U., Hirth, T. How to Ignite an Atmospheric Pressure Microwave Plasma Torch without Any Additional Igniters. *J. Vis. Exp.* (98), e52816, doi:10.3791/52816 (2015).)

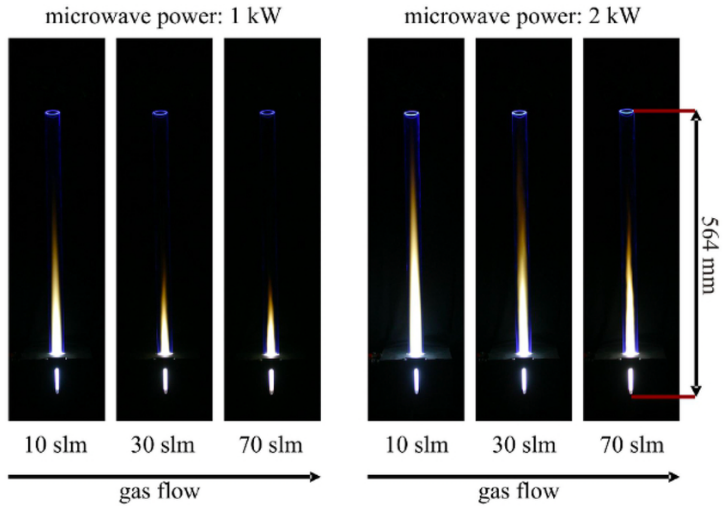

Figures 3A-B. Height of atmospheric plasma jet launched by a flattened-waveguide atmospheric pressure air plasma jet as the microwave power was varied at the fixed plasma gas flow rates of (A) 10 $slmin^{-1}$ and (B) 20 $slmin^{-1}$.

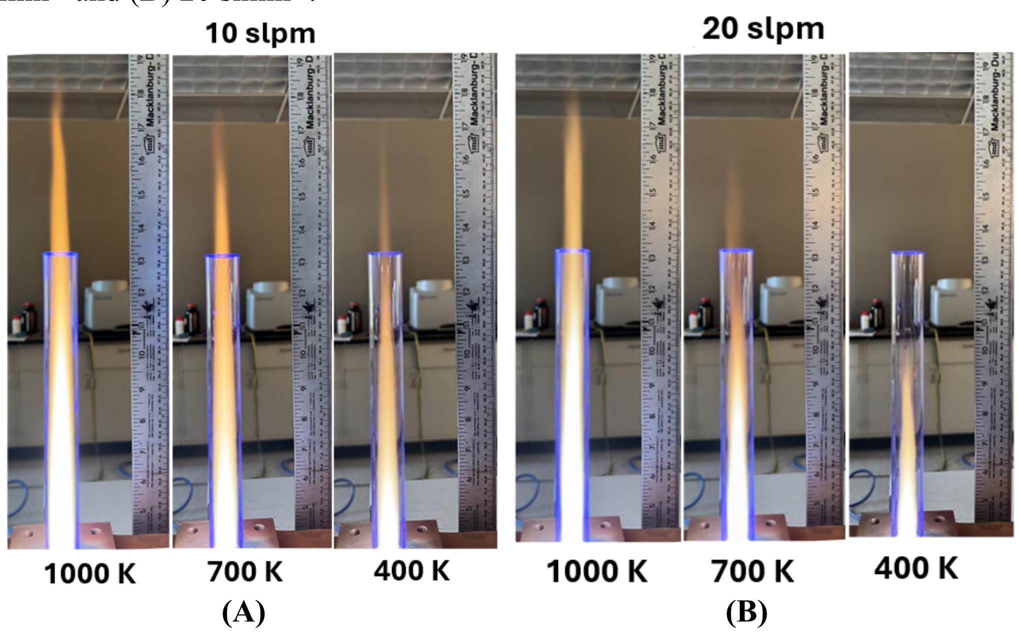

The conventional explanation of extended atmospheric plasma jets outside of the region wherein the microwave power is applied such as inside of the high-field resonator comprising a waveguide or cavity is that the microwave power transfers from the resonator to an into the external dielectric tube wherein the plasma maintained by the high internal field acts as an antenna to affect the power transfer and the microwave power propagates along the tube wall. However, atmospheric pressure plasmas such as those of air, argon, oxygen, nitrogen, CO_2, and H_2O with a typical electron density of 10^{21}-10^{23} m^{-3} cannot serve as an antenna to launch a plasma jet via a surfawave since (i) the 2.45 GHz microwave frequency is over 2000 times below the plasma cutoff frequency ω_p given by

$$\omega_p = \sqrt{\frac{N_e e^2}{m_e \varepsilon_o}} = 5.5\ X10^{12}\ Hz \tag{1}$$

where N_e is the electron density (10^{22} m^{-3}), e is the elementary charge, m_e is the electron mass, and ε_o is the vacuum permittivity, (ii) surfawaves are not sustainable due to plasma instabilities, (iii) the dielectric tube wall is nonconductive such that it could not support a traveling transverse wave, (iv) the electron temperature and density are the highest in the center and decrease radially from the center indicating the plasma is not driven from perimeter walls [14], (v) diverting power from the resonator would cause the resonator plasma to extinguish due to field loss through power conservation and lowering of the Q of the resonator, (vi) there is no plasma dielectric interface to propagate a surfawave since a gas vortex is created to prevent the plasma from contacting the dialectic tube and melting it though recombination heating, (vii) plasma is observed continuously outside of the dielectric tube as a free plasma jet with no discontinuity at the exit of the resonator indicating that the resonator is the power source, (viii) aperture size required for any significant microwave power leakage must be about a wavelength and the wavelength of the typical plasma torch microwave frequency of 2.45 GHz is 12.24 cm whereas the opening for the tube that supports the plasma is typically 2.54 cm, (ix) (a) using a microwave leakage detector (Mestek HT M2) in the present studies, no detectable microwave power emission was observed from the jet anywhere outside of the small fringe field zone of the waveguide including the free-standing plasma jet extending beyond the top of the plasma tube , (b) using a half-wave dipolar antenna attached to HF ANALYSER HF59B by Gigahertz Solutions® or wattmeter Я2M-66 Uhm et al. [15] and Benova et al. [14] reported no significant microwave power emission was observed from the jet anywhere outside the waveguide including the free-standing plasma jet, (c) using a microwave survey meter Leins et al. [9] reported no microwave leakage from the resonator cavity, (x) free jets launched as vertically traveling columns in the open cavity of a microwave oven and in large diameter vessels inside the microwave cavity are reported *infra.* wherein each plasma column was far from any vertical walls, (xi) the microwave power to maintain the discharge over the volume of the jet is more than the power to maintain the plasma in the waveguide or cavity based on plasma volume, electron density, and electron temperature, (xii) confinement is observed which is not achievable using a surfawave (e.g. plasma is confined at the top of an inverted microwave-transparent plasma vessel by microwave oven excitation as reported *infra*., and Leins et al. [9] cavity excitation experiment showed that light-emitting plasma is observed to eject out of the microwave cavity, the source of microwave power, and only exist in the jet consistent with being sustained by a dark cavity current of electrons and ions from the cavity, and (xiii) very significant non-thermal plasma jet lift (e. g. 46.9 kg (103.3 lbs.)) is reported *infra*. which is not possible for conventional discharge.

Microwave plasma jets such as those launched by flattened waveguides and resonator cavities support steady state plasma columns far outside of the source of microwave power that maintains the plasma in the absence of any measurable external microwave power. Regarding the jet mechanism, consider the cases of the present experiments, Ye et al. [11] flattened waveguide, and the Leins et al. [9] cavity wherein the plasma extends up to 438 mm, 600 mm, and 564 mm outside of the waveguide and cavity, respectively. In the Ye et al. experiment [11] for example, transit time of the plasma gas at the flow rate of 4 $X10^{-4}$ m^3/s (24 l/min) for the plasma volume of 2.71 X 10^{-4} m^3 is 0.67s. This is a very significance issue considering that the lifetime of an atmospheric-pressure air plasma following termination of the plasma power is less than 10 us [16]. Consider the Leins et al. [9] plasma jet. Using the diameter of the tube of 2.54 cm, the height of the plasma column of 0.564 m, and the air plasma gas flow rate of 15 sl/min, the maximum distance of travel before recombination is 4.9 microns. Both the plasma duration of at least 1.14 s (the gas flow transit time to propagate 0.564 m) and the measured plasma height in the tube of 0.564 m are a factor of 114,000 greater than possible in the absence of confinement. The plasma jet of plasma torches is not due to microwave excitation outside of the cavity or waveguide.

The plasma jets of the present study, Ye et al. [11] and Leins et al. [9] are shown to be due to the microwave-powered space drive force capable of plasma confinement and directional plasma pressure and lift. Specifically, space drive can serve as a mechanism of high-pressure plasma jets whereas the conventional explanation of surfawave propagation along a dielectric plasma tube launched by the plasma acting as an antenna is not supported or plausible. In this study (Figure 3), as well as those of Ye et al. [11] (Figure 1) and Leins et al. [9] (Figure 2), the vertical heights of the plasma jets were observed to be about linearly proportional to the microwave power and inversely proportional to flow rate. The linear dependence of the applied microwave power is consistent with the generation of a higher density of photon-absorbing free electrons and a greater flux of incident microwave photons to be absorbed. Both parameters increase the plasma pressure due to space drive. Given the finite energy inventory and very high fields of the flattened waveguide and cavity, the observation that the increased gas flow rate decreased the height of the plasma jet launched from flattened waveguides and cavity can be attributed an increase in the electron density and a proportional larger decrease in the electron temperature [17,18] wherein decrease in plasma temperature decreases the plasma jet speed and travel lifetime as shown by Eqs. (2-3) and (6-8). Turbulence introduced by the plasma gas whirl mechanism to prevent the plasma from contacting the tube wall may diminish the vertical flow directionality by partially randomizing it to dimmish the space drive lift. Thus, increased turbulence from increased plasma gas flow rate may diminish the jet height.

A particularly enlightening demonstration of space drive confinement in a microwave cavity is the video by Leins et al. [9] wherein the plasma jet that extending 564 mm outside the cavity (Figure 2) with no external measurable microwave power demonstrating that plasma confinement occurred in the external portion of the plasma tube in the absence of any other external confinement forces, such as a confinement force provided by a magnetic field. Specifically, the Leins et al. [9] video shows that an arc formed on an ignition needle, the plasma expanded and became brighter as it absorbed microwaves, and then the plasma disconnected from the cavity and existed only vertically outside the cavity, with the cavity going dark corresponding to launching a dark current. Leins et al. [9] measured the absence of microwave power outside of the waveguide which further supports that space drive is the source of confinement since it is not possible to maintain the plasma outside of the region of power application wherein the powerless plasma recombines in less than 10 us seconds [16,19].

This phenomenon can be explained by the space drive effect that acts as a plasma confinement force. In plasma physics, plasma confinement refers to the act of maintaining a plasma in a discrete volume. Confining plasma is required to achieve fusion power for example. There are two major approaches to confinement: magnetic confinement and inertial confinement. [20]. A plasma cannot be directly confined by temperature. Similarly, plasma cannot be confined by air flow such as by thermal up drafting due to local heating. The interaction of charged particles within the plasma with external forces, like magnetic or electric fields is necessary to achieve confinement. The high temperature of plasma gas and high energetics of the plasma electrons and ion would otherwise cause the plasma to expand and dissipate if not contained by an external force [21].

Experiments were preformed to determine if space drive predictions could match the jet observations for the specific parameters of the experiments of Ye et al. [11], Leins et al. [9], and the present waveguide experiments. The electron density n_e and electron temperature T_e were measured to use in the plasma parameter calculations of space drive. Specifically, trace H_2O was added to the plasma gases to determine the electron density n_e and electron temperature T_e of atmospheric pressure plasma jets launched by the waveguide for air at 400W, 700 W, and 1000W at flows rate of 10 sl min^{-1} and 20 sl min^{-1} as given in Table 1. Specifically, optical emission spectroscopy (OES) was performed after Ouyang [22] using a Mightex system spectrometer equipped with a fiber optic cable. The Mightex system comprised (i) a Horiba MicroHR f/3.9 imaging spectrometer (Model: MHR-MS; Horiba 140mm Czerny-Turner spectrograph) with a fixed slit width of 25 µm and a fixed height of 1 mm, a single grating mount (Model:MHR-SGM), and a 150 g/mm ruled grating blazed at 500 nm (Model: 510-49-X36), (ii) a Mightex buffered and triggerable USB 2.0 CCD linescan camera (Model: TCE-1024-UF) with 1024 pixels of 14×14 um size per pixel, spectral range from 200 to 1000 nm, 8 bit ADC at 25 kFPS, and 40 µs minimum exposure time, and (iii) a MgF_2 window (7mm diameter, 2mm thickness) on the entrance to the spectrometer and a fused silica window on the entrance of the camera. With the assumption that the ionic and atomic levels in the plasma satisfy the partial LTE (pLTE) condition, the electron temperature was determined from the Boltzmann plot. The electron density was measured by the Stark broadening of H_β lines at 486.1 nm due to its strong Stark broadening effect and weak self-absorption.

In an expanding plasma, a charge separation of electrons and ions occurs due to the electrons having much larger velocities as compared to ions. A portion of the electrons escape beyond the main plasma body that leads to the formation of a layered structure of the plasma with an external electron-rich layer (negative space charge) followed by an ion-rich layer (positive space charge) called a double layer (DL) that generates an ambipolar electric field [23]. Similarly, due to the higher electron mobility within a plasma, electrons partially separate for their positive ion pair that maintains the electrical neutrality of the plasma. The positively charged ions are accelerated toward the traveling electrons and the electrons are consequentially slowed down as some electron kinetic energy is then transferred to the kinetic energy of the ions. This process is known as ion dragging. To calculate the effects of space drive, unidirectional ions pairs much be considered.

The measured electron density n_e and electron temperature T_e were used to calculate the plasma sound speed and the plasma pressure which are made directional by space drive, and these parameters were used to determine the maximum plasma jet heights under different power and flow conditions as well as the maximum weight liftable due to the corresponding space drive force. The plasma sound speed v is given by the equation of Jones [24,25]:

$$v_e = \sqrt{\frac{\gamma_e Z k_B T_e + \gamma_i Z k_B T_i}{M}} = \sqrt{\frac{k_B T_e + 3 k_B T_e}{0.2 M_{O_2} + 0.8 M_{N_2}}} \tag{2}$$

where k_B is Boltzmann's constant, the electron temperature T_e and the ion temperature T_i are equal since they propagate as electron-ion pairs with the ions dragged by the electrons, M is the mass of air plasma constituents, nitrogen and oxygen ions, weighted by their relative atmospheric composition, γ_e is taken to be unity considering that the thermal conductivity of electrons is large enough to keep them isothermal on the time scale of ion acoustic waves, and γ_i is taken to be 3, corresponding to one-dimensional motion.

The plasma pressure is given by the product of the electron density n_e, Boltzmann's constant k_B, and the electron temperature T_e:

$$P_{plasma} = n_e k_B T_e \quad (3)$$

Space drive creates to one-dimensional electron-ion motion by orienting the plasma pressure to be in the direction of bias of the initial flow, which in the cases of the plasma jets of the present study, Ye et al. [11] and Leins et al. [9] is vertical. The space drive lift F_{plasma} is calculated by the product of the plasma pressure P_{plasma} and the area A perpendicular to the one-dimension motion axis which stops the motion.

$$F_{plasma} = P_{plasma} A \quad (4)$$

According to the kinetic theory of gases, the kinetic energy K for one directional degree of freedom f corresponding to the vertical directionality and one-dimensional motion of space drive (i.e. f =1) is related to the pressure P_{plasma} (force/area) per volume V by

$$P_{plasma} = \frac{2K}{fV} = \frac{2P_{\mu wave} t_e}{fV} \quad (5)$$

wherein the kinetic energy input to the lift K is given by the product of the microwave power applied to the plasma P_{uwave} and the space drive excitation time t_e:

$$K = P_{\mu wave} t_e \quad (6)$$

Using the plasma pressure P_{plasma} calculated using n_e and T_e (Eq. (3)), the plasma power P_{uwave}, and the volume of the tube inside of the waveguide or cavity V, the space drive excitation time t_e can be determined from Eq. (5):

$$t_e = \frac{P_{plasma}}{2P_{\mu wave}} V \quad (7)$$

Taking the space drive de-excitation time to be equal to the excitation time, the product of the plasma sound velocity v and the excitation time t_e of the space drive lift gives the jet height h_e in the absence of microwave power applied to sustain the plasma external to the flattened waveguide or cavity wherein the recombination time is otherwise typically under 10 us [16] corresponding to a height of less than a millimeter:

$$h_e = v t_e \quad (8)$$

The calculated values for P_{plasma}, v, and h and F, and the experiment results for n_e, T_e, and h_e are given in Table 1 for the applied powers of 400W, 700 W, and 1000W at flow rates of 10 sl min^{-1} and 20 sl min^{-1}. Comparing the calculated and the experimental values given in Table 1 indicates that the jets can be made more extended with further optimization to improve the efficiency. However, even the current systems are reasonably efficiency. Moreover, the lift that Ye et al. [11] and Wright et al. [13] assigned to thermal pressure is reasonably close to the space drive lift. For example, Ye et al. [11] measured about 1 kg or lift which matches the predicted value for the measured plasma pressure and the plasma tube area 1000W (Table 1).

Tables 1A-B. Electron density n_e, election temperature T_e, plasma pressure, and plasma jet height of the flattened-waveguide atmospheric pressure air plasma jet as the microwave power was varied. (A). The plasma gas flow rate was maintained at 10 sl/min. (B). The plasma gas flow rate was maintained at 20 sl/min.

Microwave Power (W)	n_e (10^{17} cm^{-3})	T_e (eV)	P_{plasma} (X 10^4 Nm^{-2})	P_{plasma} (atm)	Calculated Jet Height (mm)	Observed Jet Height (mm)	PV Work Jet Height (mm)	Lift (kg)	Pressure Velocity (m/s)
400	1.80	0.35	2.02	0.200	420	386	5.7	0.35	2165
700	1.91	0.41	2.51	0.248	565	432	9.9	0.43	2344
1000	1.95	0.46	2.87	0.284	686	483	14.2	0.50	2482

(A)

Microwave Power (W)	n_e (10^{17} cm^{-3})	T_e (eV)	P_{plasma} (X 10^4 Nm^{-2})	P_{plasma} (atm)	Calculated Jet Height (mm)	Observed Jet Height (mm)	PV Work Jet Height (mm)	Lift (kg)	Pressure Velocity (m/s)
400	2.90	0.20	1.86	0.184	292	229	5.7	0.32	1637
700	3.98	0.23	2.93	0.290	495	419	14.9	0.51	1755
1000	4.50	0.27	3.89	0.385	712	457	14.2	0.67	1902

(B)

The pressure-volume-work height of the plasma jet h_{PV} may be calculated from the pressure volume (PV) work E to extend the plasma being the energy to launch the jet, the area of the plasma tube A, and the plasma pressure P_{plasma} calculated using n_e and T_e (Eq. (3)). Specifically, multiplying the microwave power of applied to the plasma P_{uwave} and the space drive excitation time t_e results in the energy imparted to the plasma which equated to the pressure volume work allows the calculation of the height h_{PV}:

$$h_{PV} = \frac{2}{f}\frac{P_{\mu wave}t_e}{P_{plasma}A} \tag{9}$$

where P_{uwave} is the microwave power, P_{plasma} is the plasma pressure, A is the cross-sectional area, and f =3 corresponding to 3 degrees of freedom for thermal motion. The plasma jet heights determined using two methods, the product of the plasma-pressure-derived velocity and de-excitation time and PV work are given in Table 1. The heights deviate by large factors especially as the power increases demonstrating that space drive is a separate force and not a thermodynamic heat engine effect. This reinforces the distinction that space drive can give rise to plasma confinement akin to fields such as magnetic fields, whereas heat cannot. The divergence of the comparison also demonstrates that space drive increases with power as predicted. At 1000 W, space drive is calculated to provide 0.5 kg of lift which is comparable to the net lift over that provided by the constant pressure gas flow of Ye et al. [11] wherein the separate neutral gas thermal component is unknown since the gas temperature was not measured. That issue was addressed in the current experiments and analysis.

Wright et al. [13] reported a thermal model of the Ye et al. results [11] indicating that essentially of the power of the plasma in the tube outside of the waveguide was lost from the tube wall by convection of heat generated for plasma power dissipation in the tube that heated the tube wall. The thermal model contained several large mistakes in that there is no power applied to the plasma beyond the waveguide, the gas swirl at the inlet prevents the plasma gas from contacting the wall and heating the wall, the losses are predominantly radiative, and the measured gas heating is less than ½ that required to produce the measured pressure. Specifically, the Wright et al. [13] thermal power balance model assumes that the microwave discharge power occurs inside of the plasma tube along the extent of the plasma jet and all the lost power is thermal. In this study as well as others [9,14,15], no microwave power is recorded outside of the plasma jet launcher, such as a flatten wave guide or a cavity. Wright et al. [13] incorrectly assigned the radiation term to zero. Fully ionized fusion plasmas can lose up to 90% of the plasma power to radiation [26]. Inductively coupled plasmas are an intermediate ionization fraction case wherein the radiation makes up about 50% of the input power with most of the balance consumed in heating the apparatus [27]. Flames are plasmas of opposite extreme having low ionization fraction, but in this case as well, most of the power is lost to radiation [28]. The losses in these examples are those associated with heating of the plasma apparatus as well as the radiation losses. Considering the plasma power loss in isolation almost 100% is radiation loss. The radiation power balance over the range 250 nm to 11 um was measured in the present study with a Thor S322C power meter set at 125 cm distance from the center of the waveguide tube. The plasma power was 400W and the measured was 385 W.

The gas whirl mechanism in plasma jet devices such those of Ye et al. [11], Leins et al. [9] and the present study are specially designed and operated to prevent plasma from contacting the quartz tube wall. In the present study, the measured gas temperature indicated that about 5% of the power balance was due to all thermal mechanism, not just plasma gas heating. Moreover, most of the power loss from the recombination of the electrons and ions in the unpowered jet tube was measured to be from radiation in agreement with the maximum thermal loss of 11% as calculated by Ye at al. [12] considering 100% of the measured pressure was due to gas heating. Moreover, the atmospheric air plasma gas temperature was measured using a thermocouple. Matching the conditions of Ye et al. [11] of a flow rate of 1.5 m^3/h and an applied microwave power of 400 W, the measured temperature increase was only 26.1 °C (53.1 °C – 26.0 °C), whereas a rise of 67 °C was necessary for thermal pressure to be the source of the lift over the pressure to maintain the flow rate. The present results are consistent with those of other researchers that measured the parameters of atmospheric pressure microwave plasma jets launched by a flattened waveguide. For example, Humud et al. [17] characterized the plasma of a fattened-waveguide-launched atmospheric argon plasma jets excited by 2.45 GHz microwaves at 850W that was very similar to the apparatus and operating conditions of the present experiments. Humud reported a gas temperature measured using infrared thermometer with five values of gas flow rate (1, 2.5, 5, 7.5 and 10) liter min^{-1} that ranged from 32 °C to 60 ºC as well as an electron density in the range of 1.6×10^{17} - 2×10^{17} cm^{-3} and an electron temperature in the range of 0.15 eV to 0.23 eV wherein the latter two parameters were measured with OES. Similarly, Mohamed et al. [18] reported at temperature rise from 22.5 °C to less than 45 °C for a flow rate of 1 liter min^{-1} in an atmospheric microwave helium plasma jet and a gas temperature rise from 22.5 °C to less than 28 °C for a flow rate of 18 liter min^{-1}. These results are in line with those of this study indicating very little plasma gas heating with a corresponding low-pressure contribution. These plasma jets are so-called cold plasma jets.

Lift Experiments

Having established that the heights of atmospheric-air microwave plasma jets were due space drive confinement calculated from the corresponding one-dimensional plasma pressures that was dependent on the plasma power and flow rate, the space drive lift and effect of the plasma gas on the lift was determined for air, nitrogen, argon, and argon + 5% H_2 and compared to the predicted lift using the plasma pressure and vessel area according to Eqs. (3) and (4). The lift measurements were performed using the method of Ye et al. [11] with improvements in design to remove the pressure contributions other than those due to space drive. Ye et al. [11] reported that the gas temperature of a continuously power plasma was too high to measure the pressure in the plasma tube in response to varied applied power levels, moreover, a technique was sought to study fast pressure impulses, thus the technique of determining the balance of a maximumly weighted ball against gravity was used. Considering the plasma pressure measured in the present experiments and the extent of the plasma jet observed in these studies and those of Ye et al. [11], the space drive lift would have been significantly expended at the height where lift was measured by Ye et al. [11] using the weighted ball to occlude the gas outlet. Moreover, the system was quite complicated in that there was (i) background lift due to an elevated plasma gas pressure to maintain a desired plasma gas flow rate, (ii) a vertical temperature gradient from the launcher with no microwave power dissipated in the plasma gas, and (iii) thermal heating of the gas and plasma tube wall. The measurement of the space-drive-generated pressure was separated from any thermal component and the offset pressure component to main constant flow in a plasma tube by using a static gas system wherein the space drive lift was activated as a pulse rather than continuously that further eliminated any consequential thermal heating.

A flattened waveguide such as the ones used by Ye et al. [11], in the present studies, and the cavity used by Leins et al. [9] generate complex time-dependent electric and magnetic fields with longitudinal and transverse components comprising standing electric and magnetic waves of far and near field radiation components. Space drive requires gas ionization to form free electrons that are incident electromagnetic field comprising free photons or a superposition of photons that are absorbed directionally and reactionlessly. The corresponding transverse waves traveling at light speed comprise about 25% of the volume of the flatten waveguide and are deemed suitable to excite space drive [29,30]. To better achieve this condition of free space photons, a microwave generator, a microwave emitter, and a cavity large enough to support free photons, one having dimensions of at least a wavelength between any reflected surface, was sought. The most readily available and cost effective (~$60) source satisfying these criteria was a commercial microwave oven comprising a magnetron, an emitter waveguide, and a cavity (25.2 cm high x 35.3 cm wide x 36.6 cm deep). The microwave cavity had dimensions of about two wavelengths in all directions which enables propagation of free photons that are incident the gas molecules or atoms at the initiation point of the space drive event wherein free photons undergo multi-reflections from the chamber walls until absorbed by the electrons that are accelerated. Moreover, the thermal and gas-flow pressure aspects of the Ye et al. [11] measurements were eliminated by running pulsed measurements of the space drive lift wherein no gas flow was required, the plasma gas was at atmospheric pressure, gas heating was below detectable level and inconsequential, the lift was of an impulse nature, large, and easy to detect by wight lifted, high-speed audio and video recording, and acceleration detection.

To determine the microwave power applied to the plasma gases to analyze the lift efficiencies and corresponding plasma parameters, a series of microwave power absorption measurements were made by measuring the energy absorbed by different volumes of water over the same power application duration, and it was found the temperature rise of all volumes scaled inversely with volume indicating that the total power of the microwave oven is absorbed essentially independently of the heating volume. Using the water temperature rise, water weight, and water specific heat the power applied to arc-generated plasmas which launched the space drive lift was determined to be 330W.

Space drive requires a source of free electrons and free space photons. Free electrons may be provided by particle beam sources, such as electron beam. Alternatively, the source may comprise electrons and ions such as a plasma source. There are many plasma sources such as RF, DC, and microwave sources. Flames can also produce plasma comprised of free electrons and ions wherein the concentrations can be as high as 10^{10} cm^3 [31]. Flame electron and ion densities may be comparable with the densities of low-pressure RF and glow discharge plasmas [32] whereas for high-pressure plasmas such as atmospheric pressure one, the densities can be up to seven orders of magnitude or higher. Flame was effective at producing space drive lift and confinement reported *infra.* In the microwave oven cavity, wherein combustion is a source of upward directional plasma flow due to expansion from the fuel source, and space-drive driven free electrons and dragged ions are accelerated upward from the flame source with microwave photon absorption. However, this method was limited to cases having an atmosphere comprising a portion of oxygen. A preferred method of initiating space drive lift in the microwave oven cavity was found to be to use the magnetron-emitted microwaves to cause an arc on sharp edges of aluminum foil wherein the arc provided the required free electrons. Because the intensity pattern of the microwaves in the oven cavity was unknown relative to the sharp edges of the foil, it was found that reproducible and reliable initiation was achieved by mapping the microwave field and placing the foil at a at least one position where the arc was generated.

Specifically, the initiation of plasma during the present experiments was observed as an arc on serrated aluminum foil followed by brightening and expansion upward of the plasma to produce a lift impulse as the plasma traveled to the top of a quartz plasma vessel comprising an inverted or non-inverted microwave transparent quartz vessel such that the top was closed by the vessel in the inverted orientation and closed by a quartz plate in the non-inverted orientation. It was observed that plasma was tightly confined as a layer at the top (Figure 4) for very long periods of time (e.g. more than minutes). The plasma confinement occurred in the absence of any other external known confinement force such as one provided by a magnetic field. Specifically, plasma was generated in the microwave oven cavity with an initiation by an arc formed on a serrated crumbled piece of aluminum foil placed on a mica sheet that was incident microwaves wherein the mica sheet was placed on the glass carousel plate of the oven (inverted vessel experiments) or on the quartz vessel base (non-inverted vessel experiments). It was observed that the plasma traveled ballistically to the top of a closed top quartz plasma vessel and was confined to the top of the vessel. First, the metal edges of the foil concentrated the microwave electric field and caused a plasma spark. The arc served as a vertically directional source of plasma flow due to expansion from the source with intensification of the vertical plasma flow via further microwave absorption. Directional flow in the presence of microwaves incident the free electrons of the plasma caused the electrons to be accelerated upward by space drive. The vertical plasma flow was terminated on the top of the inverted vessel or cover plate, and the plasma then became confined in steady state in a volume of about 10% of the total vessel volume.

Figure 4. Ar-H_2 (5%) plasma initiated in a microwave oven cavity that traveled ballistically to the closed end of the plasma vessel where the driving space drive force achieved confinement of the plasma for very long periods of time more than minutes.

The confinement cannot be achieved thermally or by gas flow. Rather an external force is required wherein space drive provides the required force in the absence of any alternative source. Specifically, plasma recombines on the walls at the top of the inverted vessel to form neutral gas. The neutral gas flows away from the walls to mix with the bulk neutral gas driven by entropy. A confined plasma is maintained in the space at the top of the inverted vessel due space drive that acts as a net vertical force on electrons and dragged ions. Specifically, an ambipolar electric field forms due the much greater mobility of free electrons compared to ions with a bias in the negative direction predominantly at the plasma edges interfacing gas since the possible sheath at the glass interface is at least partially neutralized by recombination on the walls. The resulting bias ambipolar field favors a vertical electron drift. Once the directional flow is established the incident microwave photons accelerate the plasma free electrons in the same upward direction via space drive and drag ions to further propagate the recombination on the walls. In addition, the space drive driven light-emitting plasma and dark current flow outside of the confinement volume also supports the confinement. The upward space drive pressure is balanced by the downward neutral gas recombination pressure gradient to maintain steady state confinement. The neutral gas pressure gradient is evident as a dark space of about 5mm thickness along the wall surfaces of the confined plasma.

High speed video and sound recordings were performed to determine the temporal relationship between the production of plasma at the base of the vessel and the production of the plasma confinement. Additionally, lift was observed as initially evidenced by rattling of the vessel in the inverted position due to it being lifted from the carousel plate. As reported *infra.* the lift force was quantified by observing the ability to lift increasing weight loaded on a quartz cover plate of the vessel placed in a non-inverted orientation. The space drive lift was observed to have the characteristics of a shock wave. Using Eq. (2) to calculate the plasma sound speed from the electron temperature confirmed that it exceeded sound speed as shown in Table 2. Light emission was observed only at the location of the arc that launched a faint ballistically vertically traveling flash of plasma that became bright upon impact with the top plate followed by bright continuous emitting confined plasma wherein the electron and ion temperatures were too low to excite the background gas into a light emitting excited state during vertical propagation. The greatest lift occurred upon impact of the plasma flash with the top cover. These observations are consistent with the mechanism whereby microwave accelerated electrons that are initially moving in the upward direction drag ions and comprises a dark current. A dark current and ionization also occurs in the Crook's dark space of glow discharge cells wherein positive ions accelerate toward the cathode and electrons accelerate toward the anode compared to the space drive upward acceleration of electrons and ions as pairs. The electrons do not recombine with the dragged ions due to the separation force of the space drive effect. The charge separation is also observed at the edge of an expanding plasma that produces an ambipolar electric field as discussed *supra.* [23].

The maximum space drive lift of atmospheric pressure plasmas of the gases air, nitrogen, argon, and argon + 5% H_2 in response to 330 W of applied microwave power was determined by measuring the maximum weight lifted after the method of Ye et al. [11]. The plasma vessel comprised a right cylindrical quartz beaker, 152.4 mm ID, 152.5 mm height, 4 mm wall thickness, having a lapped-flat rim (+/- 0.05 mm) at the opening. The air experiments were performed in ambient atmosphere. The argon and nitrogen experiments were performed with a 10-times volume argon or nitrogen exchange purge of the microwave cavity and plasma vessel. The argon + 5% H_2 experiments were performed in a two-man glovebox (VAC Genesis part number 109035) wherein the gas was added through at 1.6 mm OD, 0.75 mm thickness, 305 PSI WP polyethylene line run between weight plates that were supported by ceramic spacers to form a channel for the plasma gas/vacuum line that was connected to a sealed penetration on the quartz plate covering the top of the plasma vessel. The plasma vessel was sealed with a Buna gasket with a slight coating of high-vacuum grease between the lapped-flat rim and the quartz cover plate. A second sealed-in polyethylene tube penetrated the quartz cover plate and passed through the channel in the weights and the microwave oven cavity wall through a small penetration juxtaposed with the plasma gas/vacuum line. The latter line was connected to a pressure gauge and then passed through a vacuum tight bulk-head fitting in the glove box wall. The vacuum line connected externally to a double-valved T that was connected to a vacuum pump and an argon + 5% H_2 tank. To satisfy the requirement that the initial plasma gas pressure was an exact match to the ambient atmosphere the external end of the second line was connected to either a Cali-5-Bond™ gas sampling bag (Calibrated Instruments, Inc., GSB-P/0.50, Pillow, 0.5 liter, 52 mm X 203 mm) with a threaded lock off valve that served as an indicator of a pressure balance between the plasma vessel and ambient atmospheres. A crumbled piece of aluminum foil (0.016 mm thick) was placed on a mica sheet that was placed inside of a 15.25 cm ID X 15.25 cm height, X 4 mm thick quartz cylindrical plasma vessel placed in the center of the standard rotating carousel in a non-inverted orientation inside of a commercial microwave oven. The plasma vessel was evacuated, and the high vacuum was confirmed by observing the pressure to be unchanged upon standing with the vacuum pump off for 10 minutes. Vacuum pumping was again applied after the leak test, and then plasma gas was added back until the sample bag just started to expand to achieve a match between the ambient pressure and the plasma vessel plasma gas pressure.

The open end of the plasma vessel with a lapped rim was closed by the cover plate, and nine 20 cm OD X 0.6 cm thick flat circular quartz plates were stacked on the cover plate to add weight. A 9.2 cm OD X 3 cm height machined ceramic disc was placed on the quartz plates to which was mounted a 9 cm OD plastic mount with a center bored 1.27 cm diameter hole into which a microwave transparent 1.27 OD hard wood rod inserted. The rod shaft passed through a 1.29 cm ID X 3.8 cm height tube extension of a centered penetration on the top of the oven that was welded to the top by a 3 cm OD flange. A bearing (Xike Model UC201-8 ½ inch shaft diameter) was secured on the opposite end of the rod shaft by Allen screws of the bearing collar.

Weights were loaded onto the top side of the bearing wherein the bearing permitted the free rotation of the weights to center them. The oven carousel rotational motor was deactivated. The weights comprised a series of stacked cement bricks stacked on the bearing and centered. Three sizes of cement bricks were used to determine the maximum weight of the space drive lift, 19 cm X 9.6 cm X 5.7, ~2.1 kg, 30.5 cm X 30.5 cm X 3.81 cm, ~7.73 kg and 39.4 cm X 19 cm X 3.625 cm, ~14.9 kg. When the microwave oven was turned on sparks formed on the aluminum foil which created a plasma that immediately caused a lift effect as evidenced by the lifting and rattling of the weight assembly. Bricks were sequentially added to provide a desired weight on the top of the plasma vessel plate. Weight was added until both the lift and rattle effects were suppressed. The weights were determined with a scale an accuracy to 0.1g. The high-speed video and decibel recordings of the rattling assisted in fine tuning the end point of the weight addition. The lift endpoint was also confirmed by use of a vibration detector.

The theoretical lift was calculated using the plasma pressure given by the product of the electron density n_e, Boltzmann's constant k_B, and the electron temperature T_e according to Eq. (3). The experiment results for n_e, T_e, and P_{plasma} for air, nitrogen, argon, and argon + 5% H_2 plasma are given in Table 2. Using the plasma pressure and the area of the plasma vessel (Eq. (4)), the corresponding theoretical force or lift was calculated in kg and lbs. as given in Table 2 with the corresponding measured lifts. Comparing the calculated plasma pressure lift to the weight-loading measured lift it can be appreciated that they are about the same indicating that space drive has the effect of converting the omnidirectional plasma pressure into directional pressure and force along the direction of plasma flow, the vertical axis in this case.

Table 2. Electron density n_e, election temperature T_e, plasma pressure and space drive lift of atmospheric pressure plasma jet gases air, N_2, Ar, and Ar + 5% H_2 with 330W microwave oven magnetron input power.

Plasma Gas	n_e (10^{17} cm^{-3})	T_e (eV)	P_{plasma} (10^4 Nm^{-2})	P_{plasma} (atm)	Calculated Lift (kg/lbs)	Observed Lift (kg/lbs)	Pressure Velocity (m/s)	Input Energy (J)	Lift Energy (J)	Space Drive Efficiency (%)
Air	1.28	0.19	0.779	0.0771	14.6/32.1	12.2/26.8	1595	8.25	5.8	71
N_2	1.96	0.19	1.19	0.118	22.3/49.1	15.5/34.0	1595	8.25	7.4	90
Ar	1.80	0.21	1.21	0.120	22.7/49.9	21.4/47.0	1677	13.2	10.3	78
Ar + 5% H_2	1.77	0.60	3.40	0.337	63.7/140.1	47.0/103.3	2835	13.2	11.0	84

The measured electron densities and electron temperatures given in Table 1 and Table 2 are consistent with the results of others. For example, using Stark broadening Humud et al. [17] recorded an electron density on atmospheric argon plasma jets excited by 2.45 GHz microwaves in the range of 1.6×10^{17} - 2×10^{17} cm^{-3}. Zhong et al. [33] calculate an electrons density of over 10^{16} cm^{-3} and an electron temperature of 1.3 eV on a 2.45 GHz self-excited atmospheric pressure argon microwave plasma jet capable of forming at 20 W whereas 110W is required with air substitution as the plasma gas. Using Stark broadening Mohamed et al. [17] recorded an electron density on atmospheric helium plasma jets excited by 2.45 GHz microwaves in the range of 3.5×10^{17} - 4.7×10^{17} cm^{-3}. An electron density of 7×10^{17} cm^{-3} was measured by Zhang et al. [34] on a microwave helium plasma torch at atmospheric pressure by a Mach–Zehnder interferometer.

As in the case of the waveguide, the plasma sound speed can be calculated from the electron temperature wherein the plasma sound speed permitted the calculation of the height of the flattened waveguide plasma jet in the Plasma Jet Experiments section. The plasma sound speed (Eq. (2)) was also calculated for the microwave oven cavity experiments as given in Table

2. The speed is a vertical vector that demonstrated that the maximum velocity of the space drive force is supersonic. A sonic boom was present at the point of maximum lift by the space drive pressure impulse indicating the production of a shock wave. In other applications wherein it is desirable to form a shock wave, a sufficiently high space drive plasma temperature is created with sufficient electron density such that the corresponding velocity is greater than sound speed in the plasma gas (e.g. greater than 343 m s^{-1} for air at STP), and the plasma pressure is above the threshold to achieve a desired effect.

Using high speed video, high speed audio, and accelerometer recordings of the impulse event, the excitation time of the plasma impulse and the duration time of the lift vibrations were measured to facilitate the determination of the impulse energy efficiency. The lift input kinetic energy K is given by the product of the excitation time t_e and the microwave power applied to the plasma P_{uwave} given by Eq. (7). The cover plate on the plasma vessel was thrust open upon impact of the ballistic lift impulse so the energy of lift event E_g could not be measured by the vertical height h_g that the weights were lifted. However, the lift force was against gravity, so the recorded time of the lift event t_g was used to calculate the corresponding vertical height h_g:

$$h_g = \frac{1}{2} g t_g^2 \tag{10}$$

where g is the acceleration of gravity. Then, the energy to lift the weights an equivalent height h_g is given by

$$E_g = M g h_g \tag{11}$$

where M is the mass of the weights lifted. The space drive efficiency was greater than 75% in most cases as shown in Table 2.

Consider the height predicted from an equivalent thermal pressure-volume work driven expansion. According to the kinetic theory of gases, Eq. (5) gives the relationship between the kinetic energy K for one directional degree of freedom corresponding to the vertical directionality and one-dimensional motion (i.e. f = 1)of space drive and the pressure P_{plasma} (force/area) per volume V wherein the K is given by the product of the microwave power applied to the plasma P_{uwave}, and the space drive excitation time t_e. Using the measured plasma pressure, the plasma power, and excitation time for Ar + 5%H_2 plasma, the space drive excitation volume of the plasma vessel in the microwave oven cavity can be determined. Based on high-speed video, the time of excitation time of the space drive lift of 47 kg is 40 ms. Considering the 3.40 X10^4 Nm^{-2} of plasma pressure (Table 2) and the microwave power of 330 W, the corresponding volume involved in the space drive effect is about 0.776 liters of the 2.78 l or about 28% which agrees with the faint glow after excitation of the space drive dark current that travels to the top of the plasma vessel and produces a sonic boom and bright plasma emission upon recombination.

The plasma pressures and lift were lower for air plasma and nitrogen plasma than for argon plasma which reflects the lower electron densities of the former plasmas versus the latter plasma. Due to its electronegativity oxygen forms negative ions that reduces the electron density [35] and nitrogen undergoes dissociative recombination following the charge transfer between atomic ions and nitrogen molecules [36] wherein both mechanisms decrease the electron densities. Furthermore, the space drive lift is dependent on the electron density which in turn is also dependent on the plasma gas ion lifetime. Ar^+ has a much longer lifetime than molecular ions wherein typical recombination rates for Ar^+ and molecular ions are about between 2 x 10^{-6} and 3 x 10^{-6} $cm^3\ s^{-1}$ at pressures above 1 atm [37] and 10^{-7} $cm^3\ s^{-1}$, respectively. For example, the rate coefficient of dissociative recombination of H_3^+ was determined to be about 10^{-7} $cm^3\ s^{-1}$, a very common rate coefficient for many molecular ions [38]. For T < 1200 K, the recombination rates for N_2^+, O_2^+, and NO^+ ions in the ground electronic and vibrational states respectively are 2.2×10^{-7} (Te/300)−0.39 $cm^3\ s^{-1}$, 1.95×10^{-7}(Te/300)−0.70 $cm^3\ s^{-1}$, and $(3.5 \pm 0.5) \times 10^{-7}$(Te/300)−0.69 $cm^3\ s^{-1}$ [39].

Consider hydrogen addition to argon. In a plasma, lighter ions are generally easier to drag than heavier ions by external forces like electric or magnetic fields. This is because lighter ions have less mass and therefore less inertia, meaning they resist changes in motion less than heavier ions, so they are more easily accelerated [23]. The speed and degree of confinement of the space drive force is influenced by the propensity of the ion to participate in ion dragging by the microwave accelerated electrons. For example, the mass to charge ratio of each of Ar^+, N_2^+, and H_3^+ of argon, air, and hydrogen plasmas is 40, 28, and 3, respectively, wherein the benefit of the presence of H_3^+ is evident.

Among H^+, H_2^+, and H_3^+, H_3^+ has the highest concentration in hydrogen plasma especially at high pressure wherein the concentration of H_3^+ increases lineally with hydrogen pressure [40]. This is due to the increased likelihood of collisions between ions and molecules, leading to the formation of H_2^+. While H^+ is a proton and readily combines with other molecules, and H_2^+ is a relatively short-lived species, H_3^+ is more stable due to its three-center, two-electron bonding system. At higher pressures and densities, these collisions become more frequent, increasing the concentration of H_3^+. The lower mass ion H_3^+ is the most favorable candidate for the ion dragging aspect of space drive especially at high pressure wherein the concentration increases, and the light ion is the most favored for rapid acceleration between frequent collisions with background neutral gas. Since space drive is dependent on the electron density, the lifetime of the ion is also and major factor.

Despite the shorter lifetime of H_3^+ compared to Ar^+ there are several mechanisms that favor an increased electron density with a low-proportion addition of hydrogen to argon over argon alone. Hydrogen has increased ionization, thermal diffusion, ion mobility, thermal conductivity, and gas dynamics, and the formation of stable ion H_3^+ that increases linearly with pressure [38,40,41]. The exact solutions of H_3^+, H_2^+, H_2, H, Ar^+, Ar, the free electron, and the photon are given by Mills [42]. In some cases, hydrogen can improve the thermal conductivity of the plasma, leading to an increase in electron density. Hydrogen's lower molecular weight compared to argon can also influence plasma parameters. In certain plasma conditions, the lower mass of hydrogen can lead to higher electron temperatures and greater mobility of charged species, further enhancing electron density. Hydrogen has a much lower ionization energy than argon being 13.6 eV and 15.8 eV, respectively, making it easier to ionize and produce electrons in hydrogen plasma rather than in argon. Hydrogen molecules can be easily excited and ionized by collisions with electrons. The corresponding stepwise ionization process further contributes to the generation of free electrons and ions. Also, hydrogen, being a simple molecule (H_2), readily dissociates and ionizes at lower temperatures, leading to a higher concentration of free electrons and ions.

To increase the electron density, a means of exploiting the long ion lifetime of Ar^+ while avoiding the shorter lifetime of H_3^+ due to dissociative recombination is to mix a small percentage of hydrogen in an argon plasma gas. The dramatic increase in the energetics of argon plasma with small additions of hydrogen is known [43]. Hydrogen molecules can be easily excited and ionized by collisions with electrons, particularly in the presence of metastable argon atoms. This stepwise ionization process further contributes to the generation of free electrons and ions. As shown in Table 2, there was a dramatic increase in n_e, T_e, plasma pressure, and lift with argon + 5% H_2 compared to argon alone. Argon + 5% H_2 is a widely used commercial welding, cutting, heating and brazing gas, AR HY5 [44], that does not detonate when mixed with air.

Next, consider the power balance and its relationship to thermal heating and a corresponding pressure. Space drive produces a dark current comprised microwave accelerated electrons and dragged ions wherein the separation due to space drive prevents recombination and absence of light emission. When the space drive plasma current impacts the physical boundary at the top of the plasma vessel, it reflects, the electrons and ions recombine to emit light, and ionization maintains a steady-state confined plasma. The light emission recorded from the recombining plasma of the space drive impulse essentially matched the microwave power applied, and no thermocouple-measured temperature rise was observed at an accuracy of 0.1 °C on atmospheric air plasma that was observed to lift over 12 kg. The absence of a temperature rise can easily be appreciated when the power balance is considered. Specifically, the power applied by the microwave generator was measured by placing 500 cc of water in the center of the microwave oven to match the position of the observed plasma, and the temperature before and after was measured. Using the specific heat, the power, and the time of the microwave power was determined to be 330 W. The radiation power balance measured with a Thor S322C power meter was 322 W light. The observation that essentially all the microwave power absorbed to maintain the plasma is emitted as light during the ion-electron recombination phase following the space drive effect is consistent with the results of thermal analysis of the waveguide plasma jets. Plasma gas heating by the continuous plasma waveguide system is higher than in the microwave oven cavity pulsed system. Applying the measured total 2.4% thermal inventory of the oven system over the duration of the space drive plasma impulse of 25 ms corresponds to an input energy is 0.12 J. Using the density of air of 1.2929 g/l, the volume of the plasma vessel of 2.78 l, and the air specific heat of 1.005 J/g K, the calculated temperature rise of 0.03°C in the plasma vessel from gas heating is consistent with direct thermal measurements of the microwave oven plasma gas following a lift event of less than 0.1 °C (i. e. no increase at the detection limit of +/- 0 °C).

Moreover, thermal energy for the combustion of the aluminum foil ignition with an air plasma gas was determined by weight analysis. The weight of the aluminum, foil was weighed before and after the impulse, and there was no change in weight to the sensitivity of the scale of 10 ug. Considering the weight increased by 10 ug, and the energy of combustion of Al to Al_2O_3 of -837.8 kJ/mol, the energy release of 0.17 J which would increase the air temperature for example by the negligible amount of 0.045 °C. The lack of any contribution of chemical energy to the pressure of and lift generated by space drive was confirmed by the absence of any possible aluminum reaction with argon + 5% hydrogen plasma gas wherein the plasma was ignited with the aluminum-foil-triggered arc and demonstrated the greatest lift of any of the plasma gases tested. The vertical nature of the lift was evident in that the light-weight Al foil positioned on the mica sheet is undisturbed by the ballistic upward dark plasma flow, and the foil remained having a pristine reflective metallic surface with the absence of a dull surface-oxide coating.

Conclusion

Based on the thrust and area of a jet engine a typical generated pressure of a jet is 4×10^4 Nm^{-2} or about 40% of 1 atm [45]. The measured thrust pressure of space drive in air given in Tables 1 and 2 was comparable to the thrust density of a jet engine. Moreover, during the excitation of the space drive lift impulse the lift energy given by Eqs. (10-11) was about equal to microwave energy input to the corresponding kinetic energy (Eq. (6)) indicating a very high energy efficiency (Table 2) of converting the energy of the plasma pressure acting on the plasma vessel cover plate and weights connected to it into lift energy. The microwave power results in a dark current of accelerated electrons and dragged ions with essentially no light emission or thermal heating. However, on impact of the supersonic space drive plasma flow with the corresponding physical barrier, ions and electrons recombine on the cover surface to release the plasma ionization energy as radiation, and a large wall surface heat load is also created. As an alternative converter of directed space drive plasma flow to lift, the ions and electrons may be arrested in an MHD channel [46] wherein at least one of the plasma velocity and the magnetic field exceed values for passage of plasma flow through the channel. In the case the lift is transferred to the MHD converter, the energy inventory of the electron-ion recombination and electron rotational energy may be predominantly recovered as electricity with high efficiency [46] and the resulting neutral gas recirculated in a closed directional flow system.

The power of space drive increases with electron density which has been shown to increase with pressure to very high elevation such as over 34 atm pressure [47]. Space drive has the potential of being orders of magnitude more powerful as a closed system that can provide thrust indefinitely with electrical power provided to the drive by a SunCell wherein water can serve as the source of hydrogen fuel [48]. For example, increasing the microwave power to 1 MW electric and scaling the geometric parameters in the thrust equations (e.g. Eq. (5)) demonstrate that the corresponding space drive thrust easily increases to over 1,000,000 lbs. compared to the 40,000 lbs. of axial jet exhaust thrust of the F35. Moreover, the corresponding space drive craft is anticipated to be much smaller and lighter that the 70,000 lb. F35 [49].

Considering the microwave oven cavity results give in Table 2, this first-of-a-kind space drive prototype demonstrated a weight to power ratio lift capability of about 3 W/lb. Using Eq. (5), reasonable plasma tube dimensions, plasma gas flow rates, and microwave power parameters may be selected that can achieve better than 1 W/lb space drive lift which compares very favorably to that of Starship, 100 tons/131 GW = 655,000 W/lb. Given that magnetron can be highly efficient (e.g. 90%) and the plasma ionization energy can be substantially recovered by MHD which further serves to brake the plasma and transfer the space drive kinetic energy to an object to be propelled over 90% electrical power efficiency to propulsion can be achieved.

Compact gyrotrons of megawatt scale are used to directionally and reactionlessly accelerate fusion plasmas to increase the toroidal plasma flow current. This very efficient and large-scale continuous system costs of about $1/W microwave power. Another option is the ganging commercial microwave oven magnetrons that are typically each 1000 W at a mass-production cost of about $25. The corresponding cost of 1 MW microwave power is $25k. Consider that a human can conformably tolerate a constant space drive thrust acceleration of two times the acceleration of gravity ($g = 9.8\ m/s^2$). The corresponding travel times from Philadelphia to Tokyo Japan, and to the Moon, and Mars are 18 minutes, 1 hour 45 minutes, and 2 days, respectively. Low-cost components [6-7] to propel trans-medium, omnidirectional craft of mega-pound-scale lift are commercially available to provide unconstrained mobility to transverse the oceans, sky, and solar system.

References

1. R. Mills, The Grand Unified Theory of Classical Physics, April 2023 Edition, ISBN 979-8-218-17988-5, Library of Congress Control Number 2023905641, Chapter 3 and Chapter 4, https://brilliantlightpower.com/GUT/GUT_Volume_1/, https://brilliantlightpower.com/GUT/GUT-CP-2020-Ed-Web.pdf.

2. R. Mills, https://brilliantlightpower.com/free-electron-photon-absorption-mechanism/.
3. R. Mills, The Grand Unified Theory of Classical Physics, April 2023 Edition, ISBN 979-8-218-17988-5, Library of Congress Control Number 2023905641, Chapter 34, https://brilliantlightpower.com/GUT/GUT_Volume_3/.
4. Zgadzaj, R., Welch, J., Cao, Y. et al. Plasma electron acceleration driven by a long-wave-infrared laser. Nat Commun 15, 4037 (2024). https://doi.org/10.1038/s41467-024-48413-y; https://www.nature.com/articles/s41467-024-48413-y.
5. Rehwald, M., Assenbaum, S., Bernert, C. et al. Ultra-short pulse laser acceleration of protons to 80 MeV from cryogenic hydrogen jets tailored to near-critical density. Nat Commun 14, 4009 (2023). https://doi.org/10.1038/s41467-023-39739-0; https://www.nature.com/articles/s41467-023-39739-0?fromPaywallRec=false.
6. R. Mills, "SYSTEM AND METHOD FOR INCREASING THE KINETIC ENERGY OF A DIRECTIONAL PLASMA FLOW WITH MAGNETOHYDRODYNAMIC FLOW ARRESTING", PCT Application No. PCT/US2023/084769, December 19, 2023; https://tinyurl.com/7hmsyrh.
7. R. Mills, U.S. App. No. No. 63/512304, entitled SYSTEM AND METHOD FOR INCREASING THE KINETIC ENERGY OF A DIRECTIONAL PLASMA FLOW, filed December 22, 2022; https://tinyurl.com/mpv4buwd.
8. https://www.sairem.com/solutions-for-microwave-plasma-generation/surface-wave-microwave-plasma-sources/.
9. M. Leins, S. Gaiser, A. Schulz, M. Walker, U. Schumacher, T. Hirth, "How to Ignite an Atmospheric Pressure Microwave Plasma Torch without Any Additional Igniters", J Vis Exp. 2015; (98): 52816; PMCID: PMC4541567, PMID: 25938699 (https://www.ncbi.nlm.nih.gov/pmc/articles/PMC4541567/ and https://pubmed.ncbi.nlm.nih.gov/25938699/).
10. Muegge Gerling, Gerling Applied Engineering, Inc., P.O. Box 580816, Modesto, CA 95358-0816, USA, (https://muegge.de/en/product/atmospheric-plasma-source-ma6000a-013bb/).
11. D. Ye, J. Li, J. Tang, "Jet propulsion by microwave air plasma in the atmosphere", AIP Adv. 10, 055002 (2020), https://doi.org/10.1063/5.0005814.
12. D. Ye, J. Li, J. Tang, "Response to "Comment on 'Jet propulsion by microwave air plasma in the atmosphere'" [AIP Adv. 10, 055002 (2020)]", AIP Advances 10, 099102 (2020), https://doi.org/10.1063/5.0016674.
13. P. L. Wright, S. A. Samples, N. M. Uchizono, R. E. Wirz, "Comment on "Jet propulsion by microwave air plasma in the atmosphere" [AIP Adv. 10, 055002 (2020)]", AIP Advances 10, 099101 (2020), https://doi.org/10.1063/5.0013575.
14. E. Benova, et al., "Characteristics of 2.45 GHz Surface-Wave-Sustained Argon Discharge for Bio-Medical Applications." Appl. Sci. 2022, 12(3), 969; https://doi.org/10.3390/app12030969; https://www.mdpi.com/2076-3417/12/3/969.
15. H. S, Uhm, et al. "Application of microwave plasma torch to power plant", The Institute of Electronics, Information and Communication Engineers, https://www.ieice.org/cs/isap/ISAP_Archives/2011/pdf/%5bWeC3-7%5d%20SD01_1004.pdf.
16. Y. Ikeda, J. K. Soriano, "Microwave-enhanced laser-induced air plasma at atmospheric pressure," Opt. Express 30, (2022) pp. 33756-33766, https://doi.org/10.1364/OE.470072 https://opg.optica.org/oe/fulltext.cfm?uri=oe-30-19-33756&id=497547.

17. H. R. Humud, Q. A. Abbas, A. F. Rauuf, "Effect of gas flow rate on the electron temperature, electron density and gas temperature for atmospheric microwave plasma jet", International Journal of Current Engineering and Technology, Vol. 5, No. 6, (2015), https://www.researchgate.net/publication/342875685.
18. A. J. Mohamed, A. S. Jassim, M. K. Khalaf, "Influence of gas flow on helium microwave plasma jet at atmospheric pressure", Journal of the Nigerian Society of Physical Sciences, Vol. 4 (2) (2022) 01-10, DOI: 10.5281/zenodo.7024623.
19. O. A. Fedorovich, L. M. Voitenko, "Lifetime of electrons in dense plasma", Ukrainian Journal of Physics 62(6), July (2017), pp. 489-494, DOI: 10.15407/ujpe62.06.0489.
20. J. King (U.S. DOE Office of Science), C. Greenfield (Director of the U.S. Burning Plasma Organization), "DOE Explains...Plasma Confinement", US Department of Energy, https://www.energy.gov/science/doe-explainsplasma-confinement.
21. Y. Wu, S. Şahin, *Comprehensive Energy Systems*, Volume 3: Energy Production, Editor-in-Chief Ibrahim Dincer, Copyright © 2018 Elsevier, ISBN 978-0-12-814925-6.
22. Z. Ouyang, V. Surla, T. S. Cho and D. N. Ruzic, "Characterization of an Atmospheric-Pressure Helium Plasma Generated by 2.45-GHz Microwave Power," in IEEE Transactions on Plasma Science, vol. 40, no. 12, pp. 3476-3481, Dec. 2012, doi: 10.1109/TPS.2012.2223238, https://ieeexplore.ieee.org/document/6352927.
23. X. Yao, C. W. Schneider, N. M. Bulgakova, et al., "Double layer acceleration of ions with differently charged states in a laser induced plasma", Appl. Phys. A, Vol. 129, (2023), p. 590, https://doi.org/10.1007/s00339-023-06840-6.
24. W. D. Jones, "Sound waves in plasma – a basic phenomenon and a simple diagnostic tool", July (1967), Oak Ridge National Laboratory, Oak ridge Tennessee, https://www.osti.gov/servlets/purl/4315023.
25. https://en.wikipedia.org/wiki/Ion_acoustic_wave.
26. A. Huber, et. al., "The radiated power limit in impurity seeded JET-ILW plasmas", Nuclear Materials and Energy, Vol. 33, October (2022), p. 101299, https://doi.org/10.1016/j.nme.2022.101299, https://www.sciencedirect.com/science/article/pii/S2352179122001806.
27. A. Gleizes, "Radiative Plasma Heat Transfer", In: F. Kulacki, (eds) *Handbook of Thermal Science and Engineering*, Springer, Cham., (2017), https://doi.org/10.1007/978-3-319-32003-8_26-1.
28. S.E. Guidard, W.B. Kindzierski, N. Harper, "Heat Radiation from Flares", Report prepared for Science and Technology Branch, Alberta Environment, (2000), ISBN 0-7785-1188-X, Edmonton, Alberta.
29. P. Matthews, "Filter Basics Part 6: Waveguides and Transmission Lines", June (2022), https://blog.knowlescapacitors.com/blog/filter-basics-part-6-waveguides-and-transmission-lines.
30. C. Wolff, radartutorial.u, https://www.radartutorial.eu/03.linetheory/Waveguides.en.html.
31. A. B. Fialkov, "Investigations on Ions in Flames", Prog. Energy Combust. Sci., (1997), Vol. 23, issues 5-6, pp. 399–528, https://doi.org/10.1016/S0360-1285(97)00016-6.
32. K. Akhtar, J. Scharer, R. L. Mills, "Substantial Doppler Broadening of Atomic Hydrogen Lines in DC and Capacitively Coupled RF Plasmas," J. Phys. D: Appl. Phys., Vol. 42, Issue 13 (2009), 135207 (12pp).
33. N. Zhong, X. Wei, Y. Zhong, Y. Wang, W. Chen and K. Huang, "A Novel Self-Excited Atmospheric Pressure Microwave Plasma Jet Using Rectangular Coaxial Line," IEEE

Transactions on Plasma Science, vol. 51, no. 5, pp. 1239-1246, May 2023, doi: 10.1109/TPS.2023.3264699, https://ieeexplore.ieee.org/document/10102371.
34. Q. Zhang, G. Zhang, Guixin, L. Wang, X. Wang, S. Wang, Y. Chen, "Measurement of the electron density in a microwave plasma torch at atmospheric pressure", Applied Physics Letters, Vol. 95, Issue 20, (2009), id. 201502, https://doi.org/10.1063/1.3266923.
35. D. Dorranian, M. Alizadeh, "Effect of negative oxygen ions on the characteristics of plasma in a cylindrical DC discharge", J Theor Appl Phys Vol. 8, (2014), 122, https://doi.org/10.1007/s40094-014-0122-z.
36. Y. Wang, J. Shi, C. Li, C. Feng and H. Ding, "Effect of Nitrogen Addition on Electron Density and Temperature of Cascaded Arc Argon Discharge Plasma Diagnosed by Laser Thomson Scattering," *IEEE Transactions on Plasma Science*, Vol. 47, no. 5, May (2019), pp. 1909-1916, doi: 10.1109/TPS.2019.2892053.
37. J. M. Wadehra, J. N. Bardsley, "Calculations of ion-ion recombination rates at high pressures", Appl. Phys. Lett., Vol. 32(1), (1978), pp. 76-78; doi:10.1063/1.89846.
38. M. Larsson," Dissociative recombination of H_3^+: 10 years in retrospect", Philos Trans A Math Phys Eng Sci. 2012 Nov 13;370(1978):5118–5129. doi: 10.1098/rsta.2012.0020.
39. C. H. Sheehan, J.-P. St.-Maurice, "Dissociative recombination of N_2^+, O_2^+, and NO^+: Rate coefficients for ground state and vibrationally excited ions", Journal of Geophysical Research Space Physics, Ionosphere and Upper Atmosphere, March 14, (2004), https://doi.org/10.1029/2003JA010132, https://agupubs.onlinelibrary.wiley.com/doi/full/10.1029/2003JA010132.
40. T. R. Hogness, E. G., "The ionization of hydrogen by electron impact as interpreted by positive ray analysis", Physical Review. 26 (1), (1925), pp. 44–55. Bibcode:1925PhRv...26...44H. doi:10.1103/PhysRev.26.44.
41. https://en.wikipedia.org/wiki/Trihydrogen_cation.
42. R. Mills, The Grand Unified Theory of Classical Physics, April 2023 Edition, ISBN 979-8-218-17988-5, Library of Congress Control Number 2023905641, Chapters 13,11-12, 1-2, 10, 3, and 4, https://brilliantlightpower.com/GUT/GUT_Volume_2A/.
43. R. L. Mills, P. Ray, "Substantial Changes in the Characteristics of a Microwave Plasma Due to Combining Argon and Hydrogen," New Journal of Physics, www.njp.org, Vol. 4, (2002), pp. 22.1–22.17.
44. https://www.industrialsource.com/95-argon-5-hydrogen-ar-hy5-200-cga-350--1.
45. J. Gordon Leishman, (2022–2025), *Introduction to Aerospace Flight Vehicles*, Chp. 43, Turbojet Engines, Embry-Riddle Aeronautical University, https://eaglepubs.erau.edu/introductiontoaerospaceflightvehicles/.
46. R. Mills, M. W. Nansteel, "Oxygen and Silver Nanoparticle Aerosol Magnetohydrodynamic Power Cycle", Journal of Aeronautics & Aerospace Engineering, Vol. 8, Iss. 2, No 216, (2019), pp. 1-13, https://brilliantlightpower.com/pdf/MHD_Paper.pdf.
47. S. Joshi, et al., "Temperature and Electron Density Measurements of Laser-Induced Plasmas in Air at Elevated Pressures" Spectroscopy Letters, Vol. 44(2), March, (2011), pp. 103-112, DOI: 10.1080/00387011003758372.
48. https://brilliantlightpower.com/.
49. https://www.airandspaceforces.com/weapons-platforms/f-35/.